IRSTI 31.25.15; 31.25.19 https://doi.org/10.26577/IJBCh202518115

K. Akatan[1]*, N. Kaiyrbekov[1], A. Demeukhan[1],
A. Battalova[1], E. Shaimardan[2], M. Beisebekov[2],
F. Kholiya[3], Zh. Ibraeva[4], S. Kabdrakhmanova[3]*

[1]S. Amanzholov East Kazakhstan University, Ust-Kamenogorsk, Kazakhstan
[2]Scientific Center of Composite Materials, Almaty, Kazakhstan
[3]Satbayev University, Almaty, Kazakhstan
[4]Abai Kazakh National Pedagogical University, Almaty, Kazakhstan
*e-mail: ahnur.hj@mail.ru, sanaly33@mail.ru
(Received 4 June 2025; received in revised form 9 June 2025; accepted 14 June 2025)

Synthesis of Cellulose based Hydrogel with High Absorption Capacity

Abstract. In this work, the possibility of obtaining biohydrogels from carboxymethyl cellulose (CMC) and hydroxyethyl cellulose (HEC) using citric acid (CA) as a cross-linking agent was investigated. CMC and HEC used in the work were synthesized from microcrystalline cellulose obtained from sunflower seed husks (SFH). More specifically, local agricultural waste was used as a raw material source for the monomers used to produce the hydrogel. The chemical and crystal structures of the synthesized hydrogel were analyzed using FTIR and XRD techniques, with comparisons made to the initial monomers.The thermal stability of the synthesized hydrogel was 580°C, and the mechanical strength was 134 kPa. According to the kinetics of swelling in water, it was found that the degree of swelling in the first two hours was 500%. The hydrogel synthesized on the basis of cellulose showed high potential for use as a biodegradable composite sorbent for purification of water from heavy metals, drug delivery and protect plants from drought.
Key words: biohydrogel; carboxymethylcellulose; hydroxyethylcellulose; citric acid; swelling kinetics.

Introduction

Hydrogels are three-dimensional polymer matrices that have the ability to swell significantly in aqueous media due to the retention of a large volume of liquid in their structure without dissolution [1]. This feature determines their application in various fields – from biomedicine to agriculture, from sensor devices to substance delivery systems [2]. In recent years, growing attention has been directed toward the development of biodegradable hydrogels derived from natural, renewable resources — primarily polysaccharides such as cellulose, alginates, chitosan, and their derivatives [3].

The use of natural polymers to produce biohydrogels is associated not only with their environmental safety, but also with a high degree of biocompatibility, low cytotoxicity and availability of raw materials.

Cellulose, as the most common natural polysaccharide on Earth, is of particular interest in the context of hydrogel synthesis due to the possibility of chemical modification and cross-linking under mild conditions [4]. Such derivatives easily form gel-like structures through both physical and chemical cross-linking [5].

The physicochemical characteristics of biohydrogels directly depend on the nature of the polymer used, the method of cross-linking, the degree of substitution of functional groups and the synthesis conditions [6]. The main parameters that determine the functionality of the gel system are the degree of swelling, porosity, mechanical strength, thermal stability and degradation kinetics [7-9].

In the study, hydrogels were synthesized for drug delivery and heavy metal ion sorption in water using hydroxyethyl cellulose (HEC) and carboxylmethylcellulose (CMC) as monomers, methylene bisacrylamide (MBA) and epichlorohydrin (ECH) as cross-linking agents. According to the study results, the hydrogel using MBA as a cross-linking agent was pH sensitive, releasing 85.2% of the drug at pH 7.4. On the other hand, the hydrogel using ECH as a cross-linking agent was able to sorb up to 90% of Cu^{2+} in water within one hour. However, the use of synthetic cross-linking agents in these studies does not allow the obtained hydrogels to be fully assessed as

biohydrogels. In this regard, the possibility of using organic acids as cross-linking agents, such as citric, succinic, fumaric and malic acids, has been widely studied in recent scientific works [10-11]. The studies have established that the use of natural organic acids as cross-linking agents increases the biocompatibility of the hydrogel, its chemical and physical structural stability, as well as its sorption capacity [12-13].

Based on the results of the literature review, the development of fully biocompatible cellulose-based materials is consistent with the goals of "Sustainable Development", the study investigated the possibility of synthesizing CMC and HEC from microcrystalline cellulose (MCC) obtained from local agricultural waste and then cross-linking CMC and HEC with citric acid to obtain a hydrogel. The physicochemical properties of the obtained hydrogel were determined.

Materials and methods

Materials. The following reagents were used in this work: epichlorohydrin (99%); sodium hydroxide (NaOH, ≥98%); urea (carbamide, CH_4N_2O, ≥99%); citric acid (≥99.5%); acetic acid (CH_3COOH, ≥99%); ethanol (C_2H_5OH, 95%). All chemical reagents were purchased from Sigma Aldrich and used without further purification.

Obtaining of MCC. To obtain microcrystalline cellulose, plant raw material – sunflower seed husks (SFH) – was used. MCC was obtained based on the method of Battalova, A., et all, 2024 [14]. A sample of 10 g of SFHs was measured, and a SFH to polyacrylic acid (PAA) ratio of 1:14 g/mL was used. The mixture was subjected to continuous vigorous stirring and boiled at 90 ± 5°C in a rotary flask. After heating, the mixture was cooled using a condenser to achieve delignification. The resulting MCC was then brought to 25 ± 2°C, filtered, and washed with distilled water until neutral. Finally, it was dried at 80 ± 2°C for 6 hours until a stable weight was attained (Figure 1).

Synthesis of carboxymethylcellulose (CMC) To prepare CMC, 5 g of microcrystalline cellulose (MCC) were combined with 100 ml of 95% ethanol and 10 ml of 45% NaOH solution in a flask. The mixture was stirred at 750 rpm using a magnetic stirrer for 60 minutes at room temperature. Subsequently, 5 ml of trichloroacetic acid were added, and the reaction mixture was heated in a water bath at 60 °C for another 60 minutes while stirring. After cooling to room temperature, the mixture was neutralized to a pH of 6–7 using glacial acetic acid. The resulting product was filtered through paper and washed with 500 ml of 80% ethanol using a Soxhlet extractor for 3 hours. Finally, the synthesized CMC was air-dried at room temperature. (Figure 2).

Figure 1 – Obtained MCC sample

Figure 2 – Synthesized CMC

Obtaining of hydroxyethyl cellulose (HEC). To prepare the alkaline system, a NaOH/urea/water mixture in a volume ratio of 5:7.3:50 (ml) was added to 50 ml of distilled water and stirred for 10 minutes. The resulting solution was then placed in a freezer at –12 °C for 6 hours. After cooling, it was allowed to thaw at room temperature, and a 5% suspension of microcrystalline cellulose was prepared. While continuously stirring, 45 ml of epichlorohydrin were

gradually added to the suspension. The reaction was maintained at 25 °C for 1 hour using a magnetic stirrer, followed by further incubation at 50 °C for 5 additional hours. The final product was neutralized with acetic acid and washed with distilled water until a neutral pH of 7 was reached. The suspension was subsequently frozen for 24 hours and lyophilized at –40 °C (Figure 3).

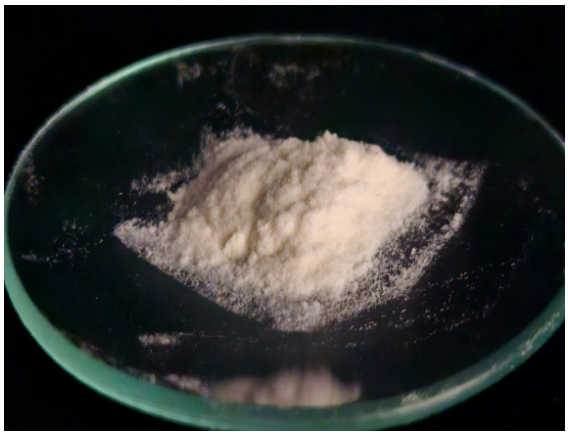

Figure 3 – Synthesized HEC

Obtaining biohydrogel. The biohydrogel was synthesized based on a mixture of CMC and HEC polymers, using citric acid (CA) as a crosslinking agent. For this purpose, a polymer solution with a total concentration of 2% by weight (relative to water) was prepared in distilled water at room temperature, with a mass ratio of CMC:HEC of 2:1, respectively. Considering the faster solubility of HEC, it was first dissolved in water, obtaining a moderately viscous transparent solution within 5 minutes. After that, CMC was added to the solution and stirring was continued for 24 hours, which resulted in the formation of a viscous homogeneous gel-like solution. Then citric acid was added to the mixture in an amount equal to 15% of the polymer composition weight. To preliminarily remove moisture, the samples were dried at a temperature of 40±2°C for 24 hours. After this, heat-induced crosslinking was carried out at a temperature of 80±5°C for the next 24 hours, with periodic monitoring of the state of the samples (Figure 4). The hydrogel synthesized during the study was conventionally designated as CMC/HEC hydrogel.

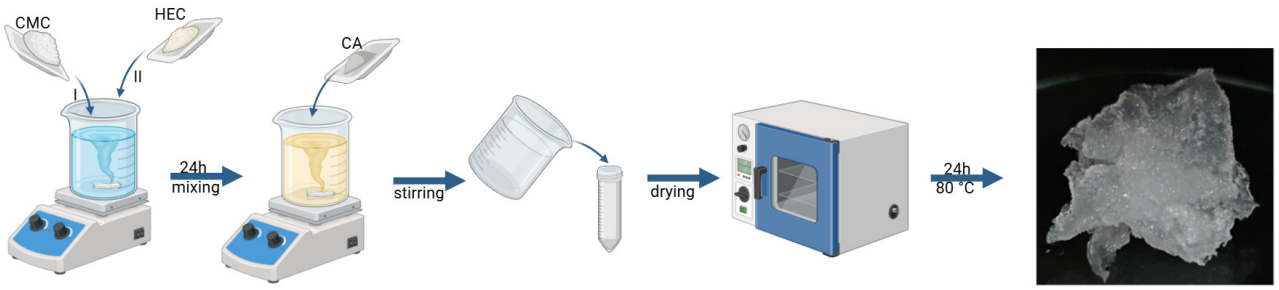

Figure 4 – Synthesis scheme of CMC/HEC hydrogel

IR-Fourier analysis. FTIR spectra were recorded using an FT-801 spectrometer (Simex, Russia) with a resolution of 1 cm^{-1} over the wavelength range of 500–4000 cm^{-1}. The standard KBr pellet method was used, with the sample and potassium bromide mixed in a 1:10 ratio. Measurements were conducted at 25°C with 100 scans per sample. Prior to use, the potassium bromide was ground and preheated at 200°C for 3 hours to remove moisture.

XRD analysis. The crystalline structures of the samples were examined using an ẌPertPRO diffractometer (Malvern Panalytical Empyrean, Netherlands) equipped with monochromatic CuKα radiation. Scanning was performed in the 2θ range of 10°–45° with a step size of 0.02°. The X-ray tube operated at a voltage of 45 kV and a current of 30 mA, with a measurement time of 0.5 seconds per step.

TGA analysis. The thermal properties of the hydrogel were investigated using a BXT-TGA 103 differential thermogravimetric analyzer (China) under an argon atmosphere. The analysis was conducted

over a temperature range of 30–700 °C, with a heating rate of 10 ± 1 °C per minute. The initial sample mass was approximately 20 ± 2 mg.

Mechanical properties. The mechanical properties of the obtained CMC/HEC hydrogel were determined by compression using a TA.XT-3000 texture analyzer (China) under standard conditions at a temperature of 25±2°C. Cylindrical hydrogel samples with a diameter of about 10 mm and a height of 10 mm were formed for testing, the surfaces of which were leveled to distribute the load uniformly. A metal cylindrical probe with a diameter of 25 mm was used as a loading element. The tests were carried out in compression mode with the following parameters: approach speed – 1.0 mm/s, compression speed – 0.5 mm/s, probe penetration depth – 5 mm or until sample failure, maximum load – up to 500N. The sample was placed in the center of the device platform, after which the probe performed a vertical movement at a given speed.

Study of the swelling kinetics of biohydrogel. Hydrogel samples weighing 0.1 g were placed in a container with distilled water at a temperature of 25±1 °C, periodically removed, excess water was removed with filter paper and weighed until a constant mass was achieved. The swelling degree (Q, g/g) was calculated as the ratio of the mass of the swollen hydrogel to the initial mass of the dry sample. The experiments were carried out in triplicate with subsequent averaging of the results. The swelling degree α was calculated using the formula:

$$\alpha\ (\%) = m\text{-}m_0/m_0*100\% \qquad (1)$$

where m is the mass after swelling of CMC/HEC hydrogel, m_0 is the initial mass of CMC/HEC hydrogel.

Results and discussion

FTIR analysis. Comparative IR spectra of the initial monomers and the synthesized hydrogel are shown in Figure 5. FTIR of CMC (Fig. 5a) is characterized by the presence of a broad band at about 3420 cm^{-1}, attributed to the stretching vibrations of hydroxyl groups (O–H), and a band at 2920 cm^{-1}, corresponding to vibrations of methylene groups (C–H) [15–17]. CMC is also typically characterized by the presence of pronounced carboxylate bands at 1640 and 1630 cm^{-1}, caused by asymmetric and symmetric stretching vibrations of $–COO^-$ groups, and a band at about 1060 cm^{-1} (C–O–C), associated with glycosidic bridges [18–19].

Figure 5b FTIR HEC revealed a broad absorption at 3358 cm^{-1} due to the O-H stretching vibration [16]. Another medium absorption band is present at 2875.57 cm^{-1} characterizing the C-H stretching vibration. The peaks at 1690 cm^{-1} and 1407 cm^{-1} were assigned to the O-H plane strain and C-H symmetric bending vibrations respectively in $-CH_2O$ [19]. Moreover, the beta-(1,4) glycoside bond was indicated by the absorption band present at 930 cm^{-1}. The absorption peak at 1120 cm^{-1} is due to the C-O antisymmetric vibration [20]. Similarly, the absorption peak at 1030 cm^{-1} is attributed to the C-O-C valence vibration in the glucopyranose structure [21].

The IR spectra of CMC/HEC hydrogel showed the characteristic absorption peaks of CMC and HEC, indicating the successful preparation of the hydrogel (Fig. 5c). A slight shift of OH groups from 3350 cm^{-1} to 3450 cm^{-1} was observed in the comparative study with CMC and HEC. This indicates the successful crosslinking of CMC and HEC by citric acid to form the biohydrogel. In addition, it was noted that the signals of carboxyl and OH groups in the range of 1630–1690 cm^{-1} in the spectra of the original CMC and HEC monomers overlap with each other in the spectrum of the CMC/HEC hydrogel and shift to 1740 cm^{-1}. This is explained by a decrease in the mobility of the carboxyl and hydroxyl groups linked to each other. [22-23]. This also corresponds to the characteristic stretching band of the carbonyl group associated with the formation of ester bonds in the hydrogel network, which confirms successful crosslinking and formation of the hydrogel.

XRD analysis. Comparative diffraction patterns of the initial CMC and HEC monomers and the synthesized CMC/HEC hydrogel are shown in Figure 6. In the CMC and HEC samples, diffraction peaks were recorded at 2Ɵ 20.5° and 22.4°. This is typical for the crystal structure of cellulose II, which corresponds to hkl 110 [24]. A peak at 2Ɵ 22.4° was found in the diffraction pattern of the CMC/HEC hydrogel. It is evident that the intensity of the diffraction peak decreased by 2 times compared to CMC and HEC. This is due to the destruction of the crystalline structures of CMC and HEC during chemical crosslinking and an increase in amorphous structures. [25]. Similar results were obtained in X-ray diffraction analysis of hydrogels synthesized from commercial CMC/HEC in [9, 26] studies. It can be concluded that the increased amorphous structure of cellulose monomers can affect the free movement of polymer units in the hydrogel matrix and the free penetration of liquids into the hydrogel.

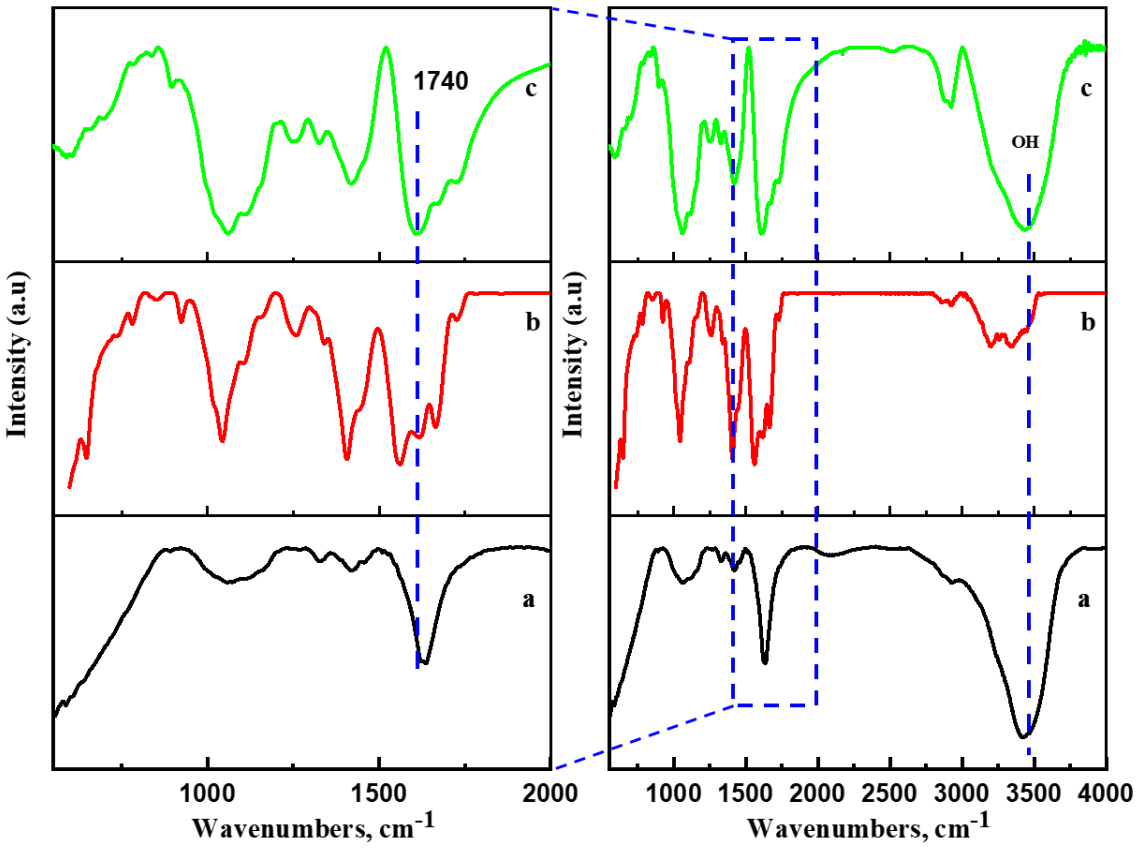

Figure 5 – IR spectra: a) CMC; b) HEC c) CMC/HEC hydrogel

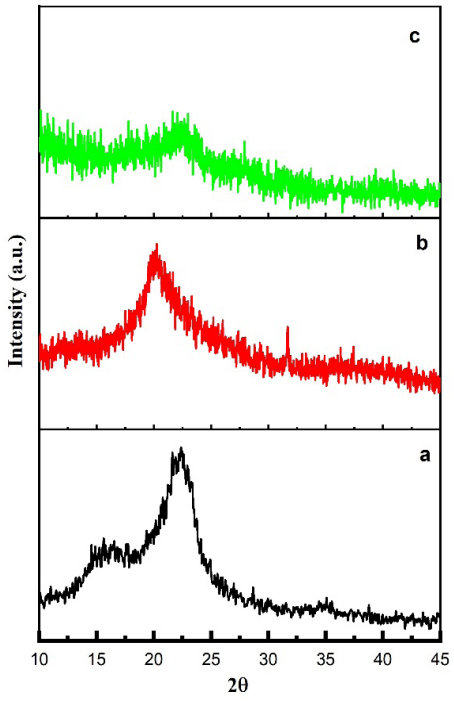

Figure 6 – XRD spectra: a) CMC;b) HEC c) CMC/HEC hydrogel

TGA analysis. TGA curves of the presented samples show differences in thermal stability and mechanisms of their thermal decomposition (Fig. 7).

TGA of CMC shows three main stages of mass loss (Fig. 7a). The first stage (up to about 200°C) is associated with the evaporation of adsorbed moisture and accounts for about 15% of the total mass. The second and most pronounced stage (200-540°C) corresponds to thermal destruction of the main chain of the cellulose polymer and decarboxylation of carboxyl groups [27, 28], the mass loss is in the range of 40-45%. The last stage of decomposition (above 400°C) is associated with further carbonization and pyrolysis of the polymer, with the formation of a small ash residue after 600°C [29].

The HEC also exhibits a three-stage thermal degradation process (Fig. 7b). The first stage (up to 200°C) is similar to CMC and involves the loss of sorbed water (~17%). The main stage (200-430°C) is accompanied by significant mass loss (~65%) due to the destruction of hydroxyethyl side groups and the main polymer skeleton [27, 30]. In the temperature range of 450°C and above, slow carbonization and

decomposition of residual organic compounds occurs with almost complete combustion in the region of temperatures of 800°C.

The hydrogel shows improved thermal stability compared to individual monomers, which is reflected in a smoother curve and a shift in the decomposition stages towards higher temperatures (Fig. 7c). At the initial stage (up to 200°C), the hydrogel does not lose mass. At temperatures of 200-580°C, 50% of the hydrogel mass undergoes degradation. This occurs due to the rupture of the main glucosidic bonds in the molecules of the original monomers and the ester bonds formed by citric acid [28]. The final stage of thermal degradation occurs at temperatures of 580-800°C. During this period, the hydrogel loses 60% of its initial mass and undergoes depolymerization. As a result, decomposition into CO_2 and other volatile organic compounds occurs. Ikrame Ayouch et. al. 2021 [22] found that the thermal stability of CMC/HEC hydrogel is 365ºC. In this study, it was found that the thermal stability of the synthesized hydrogel reaches 580ºC. This is 1.5 times higher than the previous study.

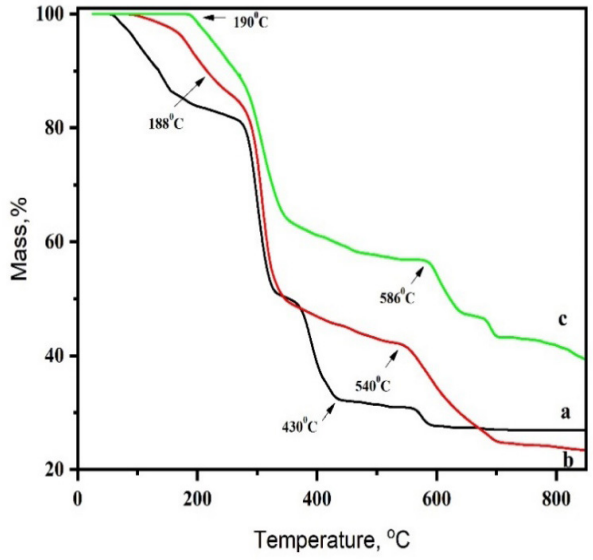

Figure 7 – TGA curves: a) CMC; b) HEC; c) CMC/HEC hydrogel

Mechanical properties of hydrogel. Figure 8 shows the mechanical strength of CMC/HEC hydrogel. The curve shows a gradual increase in stress until reaching a maximum value of about 134 kPa at 22 seconds, followed by a sharp drop, characteristic of the destruction of the material structure. This type of curve indicates the elastic-plastic behavior of the hydrogel: first, elastic deformation occurs (linear increase in pressure with a small slope), then comes the region of plastic deformation and stress accumulation (a steeper section of the curve to the maximum), after which brittle destruction of the structure occurs.

The achieved high strength index (134±4 kPa) indicates good mechanical properties of the hydrogel and points to the formation of an effective spatial network formed due to chemical crosslinking of the initial polymers. Such mechanical stability is associated with strong ether bonds that arise from the interaction of carboxyl groups of citric acid and hydroxyl groups of cellulose polymers [31]. In studies [32, 33] it was found that the mechanical strength of cellulose-based hydrogels was similar to the results obtained in this study.

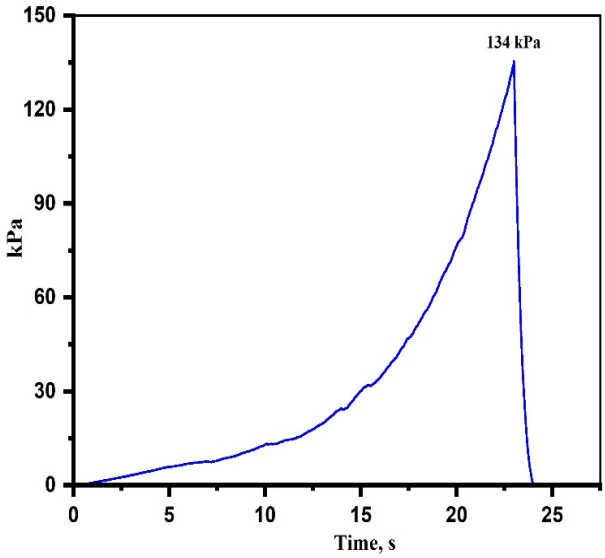

Figure 8 – Mechanical strength curve of CMC/HEC hydrogel

Study of hydrogel swelling kinetics. Figure 9 shows the kinetics of hydrogel swelling in water. The process of hydrogel swelling in water was carried out for two days until the mass stabilized. The swelling process can be divided into two stages. the hydrogel exhibited a swelling degree of up to 500±25% within the first two hours, indicating a rapid and intensive swelling process. This accelerated water absorption is attributed to the abundance of hydrophilic groups – such as hydroxyl and carboxyl – in the monomer units of the hydrogel, which pro-

mote the quick diffusion of water molecules into the polymer network [34]. In the second stage, between 2 and 30 hours, the degree of hydrogel swelling decreased by half, and the degree of swelling was 225±15%. This indicates that the hydrogel structure is compacted due to the saturation of hydrophilic groups in the monomer molecules with water molecules, and the process of water repulsion along it occurs, and equilibrium is established [35, 36]. Thus, the swelling kinetics confirms the efficiency of the hydrogel in retaining a significant volume of water, which is due to its hydrophilic nature and stable three-dimensional structure. Zhou J. et al. (2007) and Jitka Sotolařová et al. (2021) [37, 38] studied the swelling kinetics of cellulose-based hydrogels in water and obtained results similar to those of the present study.

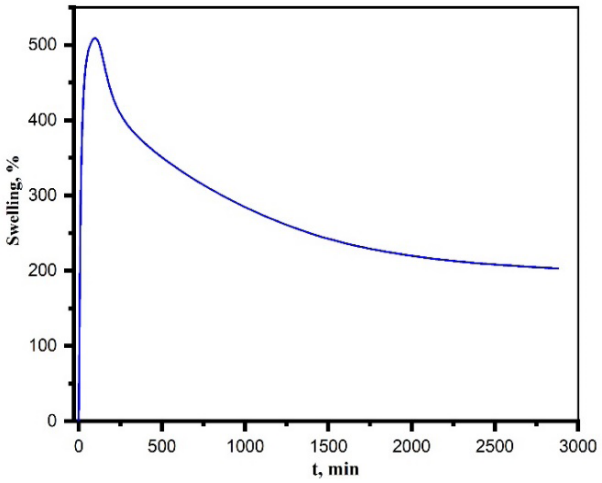

Figure 9 – Swelling kinetics curve of CMC/HEC hydrogel

Conclusion

In the course of the study, a biohydrogel based on CMC and HEC was synthesized using citric acid as a cross-linking agent. Based on the results obtained, the IR Fourier method determined that the hydrogel is cross-linked by hydroxyl and carboxyl groups of citric acid and the original monomers, CMC and HEC molecules. According to X-ray structural analysis, the crystalline structure of the CMC/HEC hydrogel has increased amorphism compared to the original monomers. The degree of swelling of the hydrogel in water reached 500% in the first two hours, and after 30 hours it decreased by 2 times, and the saturation process occurred. Resistance to external mechanical loads was 134 kPa. According to the TGA analysis, it was found that 50% of the initial mass of the hydrogel is subject to thermal degradation in the temperature range of 200-580°C, and 60% of the initial mass is lost in the temperature range of 580-800°C. Based on the results obtained, it can be seen that the CMC/HEC hydrogel has high potential for use in agricultural production as a soil conditioner to protect plants from drought, as well as for the sorption of heavy metal ions in water by immobilizing complexones in the matrix and as a carrier for the sorption of drugs in pharmaceuticals.

Acknowledgements

This research has been funded by the Science Committee of the Ministry of Science and Higher Education of the Republic of Kazakhstan (Grant No. AP23490029).

Conflict of interest

All authors are aware of the article's content and declare no conflict of interest.

References

1. Aswathy S.H., Narendra Kumar U., Manjubala I. (2022) Physicochemical Properties of Cellulose-Based Hydrogel for Biomedical Applications. *Polym.,* 14(21), pp. 4669. https://doi.org/10.3390/polym14214669.

2. Koshenaj K., Ferrari G. (2024) A Comprehensive Review on Starch-Based Hydrogels: From Tradition to Innovation, Opportunities, and Drawbacks. *Polym.,* 16(14), pp. 1991. https://doi.org/10.3390/polym16141991.

3. Manuel M., Jennifer A. (2023) A Review on Starch and Cellulose-Enhanced Superabsorbent Hydrogel. *J. Chem. Rev.,* 5(2), pp. 183-203. https://doi.org/10.22034/jcr.2023.382452.1209.

4. Sringam J., et al. (2022) Improving Mechanical Properties of Starch-Based Hydrogels Using Double Network Strategy. *Polym.,* 14(17), pp. 3552. https://doi.org/10.3390/polym14173552.

5. Ahmed E.M. (2015) Hydrogel: Preparation, characterization, and applications: A review. *J. Adv. Res.,* 6(2), pp. 105-121. https://doi.org/10.1016/j.jare.2013.07.006.

6. Thakur V.K., Thakur M.K. (2014) Processing and characterization of natural cellulose fibers/thermoset polymer composites. *Carbohyd. Polym.,* 109, pp. 102-117. https://doi.org/10.1016/j.carbpol.2014.03.039.

7. Zhao W., Jin X., Cong Y., Liu Y., Fu J. (2018) Degradable Natural Polymer Hydrogels for Articular Cartilage Tissue Engineering. *J. Chem. Techn. Biotechn.*, 93(2), pp. 403-421. https://doi.org/10.1002/jctb.3970.

8. Kadry G., Aboelmagd E.I., Ibrahim M.M. (2019) Cellulosic-based hydrogel from biomass material for removal of metals from waste water. *J. Macromol. Sci., Part A,* 61(6), pp. 419-428. *http://dx.doi.org/10.1080/10601325.2019.1640063*.

9. Wen X., Bao D., Chen M., Zhang A., Liu C., Sun R. (2015) Preparation of CMC/HEC Crosslinked Hydrogels for Drug Delivery. *BioRes*., 10(4), pp. 8339-8351. http://dx.doi.org/10.15376/biores.10.4.8339-8351.

10. Oladosu Y., Rafii M.Y., Arolu F., Chukwu S.C., Salisu M.A., Fagbohun I.K., Muftaudeen T.K., Swaray S., Haliru B.S. (2022) Superabsorbent Polymer Hydrogels for Sustainable Agriculture: A Review. *Horticulturae*, 8, pp. 605. https://doi.org/10.3390/horticulturae8070605.

11. Seki, Y., Altinisik, A., Demircioğlu, B. et al. (2014) Carboxymethylcellulose (CMC)–hydroxyethylcellulose (HEC) based hydrogels: synthesis and characterization. *Cellulose,* 21, pp. 1689-1698. https://doi.org/10.1007/s10570-014-0204-8.

12. Zhang W., Liu Y., Xuan Y., Zhang S. (2022) Synthesis and Applications of Carboxymethyl Cellulose Hydrogels. *Gels,* 8, pp. 529. https://doi.org/10.3390/gels8090529.

13. Nasution H., Harahap H., Dalimunthe N.F., Ginting M.H.S., Jaafar M., Tan O.O.H., Aruan H.K., Herfananda A.L. (2022) Hydrogel and Effects of Crosslinking Agent on Cellulose-Based Hydrogels: A Review. *Gels,* 8(9), pp. 568. https://doi.org/10.3390/gels8090568.

14. Battalova A., Ibraeva Z., Kabdrakhmanova S., Akatan K., Shaimardan E., Demeukhan A., Tursyngazykyzy A., Beisebekov M., Maussumbayeva A. (2024) Comparative characteristics of microcrystalline cellulose obtained from the rice waste production of Kazakhstan. *Chem. Bull. Kaz. Nat. Univ.,* 113(4), pp. 14-23. https://doi.org/https://doi.org/10.15328/cb1386.

15. Tang Q., Zhang Y., Li Y., Yang H. (2022) Biodegradable Hydrogels for Biomedical Applications. *Gels,* 8(11), pp. 695. https://doi.org/10.3390/gels8110695.

16. Denagbe W., Mazet E., Desbrières J., Michaud P. (2025) Superabsorbent polymers: Eco-friendliness and the gap between basic research and industrial applications. *React. Funct. Polym.,* 214, pp. 106278. https://doi.org/10.1016/j.reactfunctpolym.2025.106278.

17. Fan M., Dai D., Huang B. (2019) Fourier Transform Infrared Spectroscopy for Natural Fibres. *Fourier Transf. -Mat. Anal.*, 3, pp. 45-68. https://doi.org/10.5772/intechopen.80207.

18. Kassab Z., Abdellaoui Y., Hamid M., Achaby M.El. (2020) Cellulosic materials from pea (Pisum Sativum) and broad beans (Vicia Faba) pods agro-industrial residues. *Mater. Lett.,* 280, pp. 128539. https://doi.org/10.1016/j.matlet.2020.128539.

19. Darbasizadeh B., Fatahi Y., Feyzi-barnaji B., Arabi M., Motasadizadeh H., Farhadnejad H., Moraffah F., Rabiee N. (2019) Crosslinked-polyvinyl alcohol-carboxymethyl cellulose/ZnO nanocomposite fibrous mats containing erythromycin (PVA-CMC/ZnO-EM): Fabrication, characterization and in-vitro release and anti-bacterial properties. *Int. J. Biol. Macromol.,* 141, pp. 1137-1146. https://doi.org/10.1016/j.ijbiomac.2019.09.060.

20. Gong T., Hou Y., Yang X., Guo Y. (2019) Gelation of hydroxyethyl cellulose aqueous solution induced by addition of colloidal silica nanoparticles. *Int. J. Biol. Macromol.,* 134, pp. 547-556. https://doi.org/10.1016/j.ijbiomac.2019.05.069.

21. Kassab Z., Boujemaoui A., Ben Youcef H., Hajlane A., Hannache H., Achaby M.El. (2019) Production of cellulose nanofibrils from alfa fibers and its nanoreinforcement potential in polymer nanocomposites. *Cellulose,* 26, pp. 9567-9581. https://doi.org/10.1007/s10570-019-02767-5.

22. Ayouch I., Kassem I., Kassab Z., Barrak I., Barhoun A., Jacquemin J., Draoui K., El Achaby M. (2021) Crosslinked carboxymethyl cellulose-hydroxyethyl cellulose hydrogel films for adsorption of cadmium and methylene blue from aqueous solutions. *Surf. Interf.,* 24, pp. 101124. https://doi.org/10.1016/j.surfin.2021.101124.

23. Seki Y., Altinisik A., Demircioglu B., Tetik C. (2014) Carboxymethylcellulose (CMC)-hydroxyethylcellulose (HEC) based hydrogels: Synthesis and characterization. *Cellulose*, 21, pp. 1689-1698. https://doi.org/10.1007/s10570-014-0204-8.

24. Battalova A., Kabdrakhmanova S., Akatan K., Shaimardan E., Beisebekov M., Karzhaubayeva A., Kantay N., Ibraeva Zh., Thomas S. (2025) Synthesis and Application of Biodegradable Cellulose Hydrogels From Sunflower Husks as a Water□Retaining Material in Agriculture. *J. Polym. Sci.*, pp. 1-12. https://doi.org/10.1002/pol.20240486.

25. Yang S., Fu S., Liu H., Zhou Y., Xueyun L. (2011) Hydrogel Beads Based on Carboxymethyl Cellulose for Removal Heavy Metal Ions. *J. Appl. Polym. Sci*., 119(2), pp. 1204-1210. https://doi.org/10.1002/app.32822.

26. Akar E., Altınışık A., Seki Y. (2012) Preparation of pH- and ionic-strength responsive biodegradable fumaric acid crosslinked carboxymethyl cellulose. *Carbohydr. Polym.,* 90(4), pp. 1634-1641. https://doi.org/10.1016/j.carbpol.2012.07.043.

27. Luo X., Liu C., Wang Y., Huang Y., Yao J. (2020) Preparation and characterization of hydroxyethyl cellulose/poly(vinyl alcohol) composite films with improved mechanical and water resistance properties. *Cellulose*, 27(11), pp. 6535-6546. https://doi.org/10.1007/s10570-020-03221-8.

28. Demitri C., Scalera F., Madaghiele M., Sannino A., Maffezzoli A. (2018) Potential of cellulose-based superabsorbent hydrogels as water reservoir in agriculture. *Int. J. Polym. Sci.*, pp. 1-6. https://doi.org/10.1155/2018/4350734.

29. Wang M., Chen X., Zhang H., Zhang Y. (2019) Thermal decomposition and kinetic analysis of carboxymethyl cellulose based polymer electrolytes. *J. Therm. Anal. Calorim.,* 135(3), pp. 2305-2313. https://doi.org/10.1007/s10973-018-7442-2.

30. Barud H.S., de Araújo Júnior A.M., Santos D.B., de Assunção R.M.N., Meireles C.S., Cerqueira D.A., Ribeiro C.A. (2008) Thermal behavior of cellulose derivatives. *J. Therm. Anal. Calorim.,* 93(3), pp. 817-821. https://doi.org/10.1007/s10973-007-8439-1.

31. Chang C., Peng J., Zhang L., Pang J. (2021) Cellulose-based hydrogels: Preparation, properties, and applications. *Polym. Rev.,* 61(2), pp. 257-307. https://doi.org/10.1080/15583724.2020.1861143.

32. Aswathy S.H, NarendraKumar U., Manjubala I. (2022). Physicochemical Properties of Cellulose-Based Hydrogel for Biomedical Applications. *Polym.*, 14(21), pp. 4669. https://doi.org/10.3390/polym14214669.

33. Ciolacu D.E., Suflet D.M. (2019) Cellulose-Based Hydrogels for Medical/Pharmaceutical Applications. Elsevier B.V.: Amsterdam, The Netherlands. ISBN 9780444637741.

34. Li J., Mooney D.J. (2016) Designing hydrogels for controlled drug delivery. *Nat. Rev. Mat.,* 1(12), pp. 16071. https://doi.org/10.1038/natrevmats.2016.71.

35. Kabiri K., Omidian H., Hashemi S.A., Zohuriaan-Mehr M.J. (2011) Synthesis and characterization of hydrogels. *Eur. Polym. J.*, 47(2), pp. 1133-1145. https://doi.org/10.1016/j.eurpolymj.2011.02.022.

36. Peppas N.A., Sahlin J.J. (1989) A simple equation for the description of solute release. III. Coupling of diffusion and relaxation. *Int. J. Pharm.,* 57(2), pp. 169-172. https://doi.org/10.1016/0378-5173(89)90306-2.

37. Zhou J., Chang C., Zhang R., Zhang L. (2007) Hydrogels prepared from unsubstituted cellulose in NaOH/urea aqueous solution. *Macromol. Biosci.,* 7(6), pp. 804-809. https://doi.org/10.1002/mabi.200700007.

38. Sotolářová J., Vinter Š., Filip J. (2021) Cellulose derivatives crosslinked by citric acid on electrode surface as a heavy metal absorption/sensing matrix. *Coll. Surf. A: Physicochem. Eng. Aspects*, 628, pp. 127242. https://doi.org/10.1016/j.colsurfa.2021.127242.

Information about authors

Kydyrmolla Akatan – PhD, S. Amanzholov East Kazakhstan University (Oskemen, Kazakhstan, e-mail: ahnur.hj@mail.ru)

Nariman Kaiyrbekov – Junior research assistant, S. Amanzholov East Kazakhstan University (Oskemen, Kazakhstan, e-mail: narimankayrbekov@gmail.com)

Ansagan Demeukhan – Junior researcher, S. Amanzholov East Kazakhstan University (Oskemen, Kazakhstan, e-mail: demeuhanansagan@gmail.com)

Ainur Battalova – Junior researcher, S. Amanzholov East Kazakhstan University (Oskemen, Kazakhstan, e-mail: 2012kausar@mail.ru)

Esbol Shaimardan – PhD, Scientific Center of Composite Materials (Almaty, Kazakhstan, e-mail: esbol_shay@mail.ru)

Madiar Beisebekov – PhD, Scientific Center of Composite Materials (Almaty, Kazakhstan, e-mail: make1987@mail.ru)

Faisal Kholiya – PhD, Satbayev University (Almaty, Kazakhstan, e-mail: faisalkholiya91@gmail.com)

Zhanar Ibraeva – Candidate of Chemical Sciences, Associate Professor, Abai Kazakh National Pedagogical University (Almaty, Kazakhstan, e-mail: Zhanar-ibraeva@mail.ru)

Sana Kabdrakhmanova – Candidate of Technical Sciences, Associate Professor, Satbayev University (Almaty, Kazakhstan, e-mail: sanaly33@mail.ru)